Titania bicontinuous network structures for solar cell applications

H. Wang
Department of Physics, The University of Hong Kong, Pokfulam Road, Hong Kong

C. C. Oey
Department of Electrical and Electronic Engineering, The University of Hong Kong, Pokfulam Road, Hong Kong

A. B. Djurišić,[a] M. H. Xie, and Y. H. Leung
Department of Physics, The University of Hong Kong, Pokfulam Road, Hong Kong

K. K. Y. Man and W. K. Chan
Department of Chemistry, The University of Hong Kong, Pokfulam Road, Hong Kong

A. Pandey and J.-M. Nunzi
Laboratoire des Proprietés Optiques des Matériaux et Applications, CNRS UMR 6136, Université Angers, 2 Boulevard Lavoisier, 49045, Angers Cedex, France

P. C. Chui
Department of Electrical and Electronic Engineering, The University of Hong Kong, Pokfulam Road, Hong Kong

(Received 30 March 2005; accepted 25 May 2005; published online 8 July 2005)

We report fabrication of a TiO_2 interconnected network structure for photovoltaic applications, which was obtained using polystyrene-*block*-polyethylene oxide diblock copolymer as the templating agent. The synthetic method is simple and highly reproducible. The pore size of the structure is controlled by the amount of Ti precursor provided. The heterojunction solar cells consisting of a TiO_2 porous network structure and poly (2-methoxy-5-(2′-ethyl-hexyloxy)-p-phenylene vinylene) (MEH-PPV) showed improved performance with a short circuit current of 3.25 mA/cm^2 under AM 1.5 solar illumination. The achieved maximum external quantum efficiency for optimum MEH-PPV thickness was 34%. © *2005 American Institute of Physics*. [DOI: 10.1063/1.1992659]

Dye-sensitized solar cells based on TiO_2 can reach an efficiency as high as 10%.[1] In order to eliminate difficulties associated with liquid electrolyte, considerable research is devoted to the development of solid state dye-sensitized solar cells[2] or polymer-TiO_2-based solar cells.[2–12] In addition to TiO_2, other oxide materials can be used, such as ZnO.[13] While the power conversion efficiencies of solid state dye-sensitized cells can reach ~4%,[2] the efficiencies of polymer-TiO_2 solar cells are considerably lower, typically below 1% in the absence of electrolyte.[2–12] One of the problems in the development of efficient polymer-TiO_2 cells is incomplete filling of the TiO_2 pores by the hole transport material.[2] In order to control the pore size and morphology of the TiO_2 layer, TiO_2 synthesis methods using block copolymers as structure directing agents were proposed.[14–20] However, such approaches result in films in which typically ~33% of the film volume can be filled with a polymer,[14] resulting in maximum external quantum efficiency (EQE) of ~10%.[3] The shape of TiO_2 nanocrystals was also shown to affect the charge transfer between poly (2-methoxy-5-(2′-ethyl-hexyloxy)-p-phenylene vinylene) (MEH-PPV) and TiO_2 by affecting the number of available percolation paths.[21] Consequently, it is expected that improved photovoltaic performance can be obtained for TiO_2 layer morphology resulting in easy polymer infiltration and a large number of percolation pathways.

In this work, we propose a method for fabricating highly porous TiO_2 layers consisting of a three-dimensional interconnected network of anatase crystallites. Poly (styrene-*block*-ethylene oxide) (PS-*b*-PEO) was used as a templating agent, while titanium tetraisopropoxide (TTIP) was used as the TiO_2 precursor. The morphology and the average pore size can be easily changed from ~5 to ~35 nm by adjusting the TTIP concentration. The porous TiO_2 layers were used to fabricate solar cells with MEH-PPV (molecular weight 40 000–70 000 g/mol, obtained from Aldrich) as the sensitizer/hole-conducting material. There were several previous reports on the TiO_2/MEH-PPV heterojunction cells.[5–8,11] However, in all these reports, the short-circuit current was smaller than 1 mA/cm^2. Considerable improvement in the short-circuit current (3.3 mA/cm^2) was obtained in our work due to a different TiO_2 layer morphology.

The titania interconnected network was prepared as follows. A 1% w/v toluene solution of PS-*b*-PEO [Polymer Source Inc., with polydispersity $M_w/M_n=1.04$ and average molecular weight of 25 300 g/mol and weight ratio of 75:25 (PS:PEO)] was prepared and aged overnight. Solutions of 2.5% w/v TTIP (99.999%, Aldrich Chemical Co.) in toluene were prepared. The mixed solutions of PS-*b*-PEO and TTIP with different volume fractions were aged for 5 min before spin-coating on cleaned indium tin oxide (ITO) glass substrates with surface sheet resistance ~10 Ω/□. Films with different thicknesses were obtained at different spin speeds. The films were then calcined by heating at a rate of 1 °C min^{-1} to 200, 300, or 400 °C in the atmosphere (rela-

[a]Electronic mail: dalek@hkusua.hku.hk

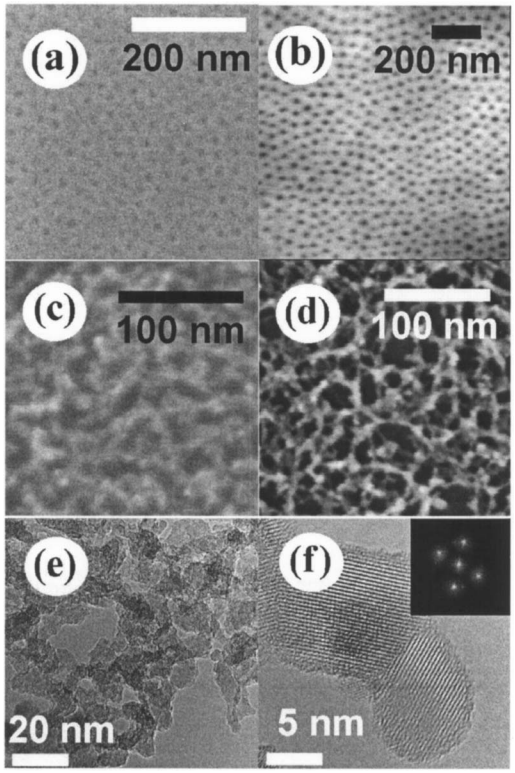

FIG. 1. Topography of PS-*b*-PEO films. (a) FESEM image, (b) AFM image, and (c) SEM images of PS-*b*-PEO and TTIP films annealed at (c) 200 °C for 18 h, (d) 400 C for 5 h. (e) and (f) TEM and HRTEM images of PS-*b*-PEO and TTIP films annealed at 400 °C for 5 h.

tive humidity ~50%) for 5 h. The field-emission scanning electron microscopy (FESEM) images were obtained using Leo 1530 FESEM. Transmission electron microscopy and high-resolution transmission electron microscopy (HRTEM) images were obtained using JEOL 2010F TEM. For investigating the solar cell performance of the fabricated porous TiO_2, solar cells with structure ITO/TiO_2/MEH-PPV/Au were prepared. Pure polymer devices with structure ITO/MEH-PPV/Al were also prepared for comparison. Both the substrates with TiO_2 films and bare ITO substrates for control devices were cleaned using UV ozone before spin-coating MEH-PPV, which improved the device performance. The solution of MEH-PPV in xylene (6 mg/ml) was then spin-coated on top of the TiO_2 films. The spinning conditions for the desired MEH-PPV thickness (before annealing) were determined by checking the thickness of layers spin-coated on glass substrates using a step profiler. The films were then baked for 15 h in a vacuum oven at 100 °C. The Au electrode (30 nm) was evaporated in high vacuum (10^{-6} Pa). The current-voltage characteristics were measured using a Keithley 2400 sourcemeter. For white-light efficiency measurements, Oriel 66002 xenon arc lamp with AM 1.5 filter was used. The light intensity was 100 mW/cm^2. For external quantum efficiency measurements, an Oriel Cornerstone™ monochromator was used. All the characterizations were performed in air.

Spin-coating of pure PS-*b*-PEO copolymer used as a template results in a film consisting of the array of PEO cylinders in a PS matrix, in agreement with previously reported results.[22] The scanning electron microscopy (SEM) and atomic force microscopy (AFM) images of the pure PS-*b*-PEO are shown in Figs. 1(a) and 1(b). PEO cylinders with

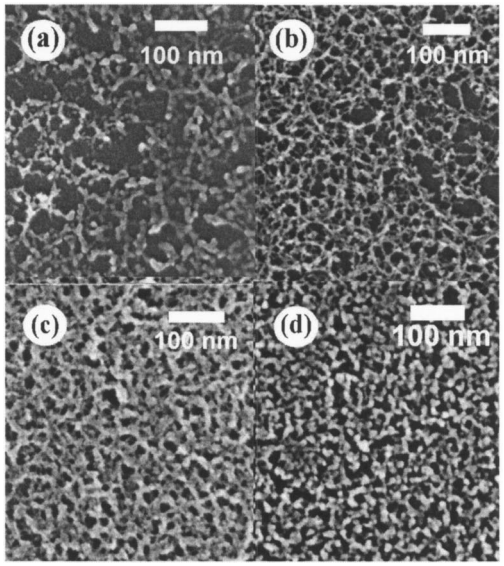

FIG. 2. SEM images of P(S-*b*-EO) and TTIP films with different TTIP concentrations annealed at 400 °C for 5 h; (a) 15%, (b) 25%, (c) 35%, and (d) 45%.

20 nm diameter and 50 nm center-to-center spacing can be clearly observed. Based on the theory of phase separation of block copolymer films,[23] it is expected that the obtained morphology would become gyroid and then lamellar with further increases of the volume fraction of PEO. When TTIP solution is mixed with the PS-*b*-PEO solution, a film with the featureless surface is obtained after spin-coating. This is expected since toluene is a good solvent for polystyrene, and the component which is preferentially solvated by the solvent used will have the tendency to appear on the surface.[24] Mixing of the TTIP and PS-*b*-PEO solutions will result in the coordination of TTIP by the PEO block, which may significantly change the conformation of the polymer. Since ethylene oxide segments are known to form crown-ether-type complexes with a number of inorganic ions,[16] the coordination will likely further decrease the solubility of the PEO block in toluene,[18] resulting in preferential segregation of the PS on the surface and possible change of the morphology inside the film. The annealing in atmosphere results in the conversion of the Ti-containing block to TiO_2 and the appearance of the interconnected network, as shown in Figs. 1(c)–1(e). The use of the thermolytic molecular precursor route was previously reported for the synthesis of mixed oxide materials,[25] but no interconnected networks were obtained. The obtained morphology shows some resemblance to the porous structure before heat treatment previously reported by Kavan *et al.*[15] using a Pluronic® P-123 template. The network structure is already visible after annealing at 200 °C, as seen in Fig. 1(c). However, annealing at higher temperatures (300 and 400 °C) is necessary to improve the crystallinity of the TiO_2. After 5 h annealing at 400 °C, the major part of the interconnected network are TiO_2 anatase crystallites, as shown in the HRTEM image Fig. 1(f). Cubic,[19] hexagonal,[19] and lamellar[20] structures were previously reported for block copolymer templated TiO_2 films. The obtained morphology of our TiO_2 network indicates the possibility that gyroid morphology served as a template, but this requires further study.

Figure 2 shows the variation in morphology and the pore size of TiO_2 obtained from TTIP solutions with concentra-

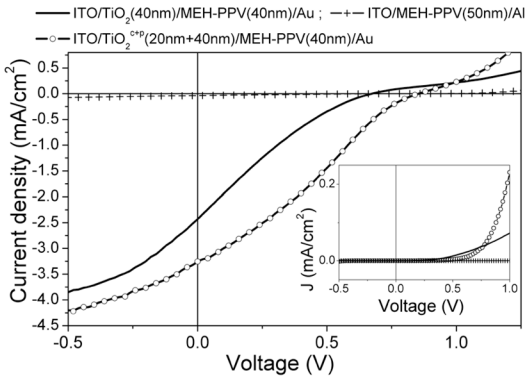

FIG. 3. Current-voltage characteristics of the TiO_2/MEH-PPV under AM 1.5 100 mW/cm^2 illumination. The inset shows *I-V* curves in the dark. The curves corresponding to an ITO/MEH-PPV/Al device are also shown for comparison.

tions from 15% to 45%. It can be observed that the pore size decreases when TTIP concentration increases. Larger pore size will result in an easier filling with the polymer, thus resulting in an increase of the short-circuit current.[12] However, lower concentrations result in inferior connectivity. Fabrication of a highly interconnected network is mandatory for achieving an efficient charge separation and transport to the electrodes due to a large number of available percolation paths. Thus, it is necessary to find a compromise between the connectivity and the pore size to improve both charge transport and pore filling. Therefore, the films obtained from 35% TTIP solutions were identified as the most promising for device applications and they were used for the fabrication of solar cells. The TiO_2 film thickness measured from cross-section SEM image was 40 nm. The average pore size in these films is ~23 nm [see Fig. 2(c)].

Figure 3 shows the obtained current-voltage characteristics of ITO/TiO_2/MEH-PPV/Au devices for a 40 nm MEH-PPV layer with and without a compact TiO_2 layer. Without the compact layer, we obtain a short circuit current density I_{sc} of 2.4 mA/cm^2, an open circuit voltage V_{oc} of 0.68 V, and a fill factor FF of 0.19, resulting in a power conversion efficiency η of 0.29%. In order to prevent the direct contact between the MEH-PPV and the ITO electrode, a compact TiO_2 layer was prepared by annealing the films spin-coated from PEO:TTIP isopropanol solutions at 400 °C for 1 h. When a pure PEO polymer instead of a PS-*b*-PEO copolymer is used, a compact TiO_2 layer is obtained instead of a porous one. The addition of the compact layer yields considerable improvement in the device performance, resulting in I_{sc}=3.3 mA/cm^2, V_{oc}=0.86 V, FF=0.28, and efficiency η =0.71%. Both devices exhibit substantially improved performance compared with a MEH-PPV Schottky device, as expected, and the short-circuit current is considerably higher compared with the values reported in the literature for TiO_2/MEH-PPV heterojunctions. This can likely be attributed to an increased number of percolation paths in our interconnected TiO_2 network and improved pore filling. However, obtained values of the fill factor are relatively low. This would likely be improved by performing measurements in a glovebox instead of ambient, and further device structure optimization, such as doping of the MEH-PPV to improve conductivity, using a different polymer with wider solar spectrum coverage, and improving the electron-collecting contact on the ITO/TiO_2 interface and the hole-collecting contact at the MEH-PPV/Au interface. When MEH-PPV thickness is varied, the best performance (maximum EQE of 34%) is obtained for MEH-PPV thickness equal to the thickness of MEH-PPV porous layer.

To summarize, a titania interconnected network structure with large pores was obtained using PS-*b*-PEO diblock copolymer as the templating agent. The synthetic method is simple and highly reproducible. The pore size of the structure is controlled by the amount of TTIP provided. Improved performance of MEH-PPV based solar cells was obtained using fabricated porous TiO_2 films.

This work is supported by The Research Grants Council of the Hong Kong Special Administrative Region (Project Nos. HKU 7009/03P, 7008/04P, and 7019/04P and France/Hong Kong Joint Research Scheme project F-HK25/03T), and by the PROCORE program of the ministry of foreign affairs in France (No. 07799XM) and the University of Hong Kong University Development Fund Grant.

[1] B. O'Regan and M. Grätzel, Nature (London) **353**, 737 (1991).
[2] A. F. Nogueira, C. Longo, and M.-A. De Paoli, Coord. Chem. Rev. **248**, 1455 (2004).
[3] K. M. Coakley and M. D. McGehee, Appl. Phys. Lett. **83**, 3380 (2003).
[4] K. M. Coakley and M. D. McGehee, Chem. Mater. **16**, 4533 (2004).
[5] Q. Fan, B. McQuillin, D. D. C. Bradley, S. Whitelegg, and A. B. Seddon, Chem. Phys. Lett. **347**, 325 (2000).
[6] P. M. Sirimanne, T. Shirata, L. Damodare, Y. Hayashi, T. Soga, and T. Jimbo, Sol. Energy Mater. Sol. Cells **77**, 15 (2003).
[7] K. Takahashi, K. Seto, T. Yamaguchi, J.-I. Nakamura, C. Yokoe, and K. Murata, Chem. Lett. **33**, 1042 (2004).
[8] A. J. Breeze, Z. Schlesinger, S. A. Carter, and P. J. Brock, Phys. Rev. B **64**, 125205 (2001).
[9] D. Gebeyehu, C. J. Brabec, N. S. Sariciftci, D. Vangeneugden, R. Kiebooms, D. Vanderzande, F. Kienberger, and H. Schindler, Synth. Met. **125**, 279 (2002).
[10] P. A. van Hal, M. M. Wienk, J. M. Kroon, W. J. Verhees, L. H. Sloof, W. J. H. van Gennip, P. Jonkheijm, and R. A. J. Janssen, Adv. Mater. (Weinheim, Ger.) **15**, 118 (2003).
[11] M. Y. Song, K.-J. Kim, and D. Y. Kim, Sol. Energy Mater. Sol. Cells **85**, 31 (2005).
[12] C. D. Grant, A. M. Schwartzberg, G. P. Smestad, J. Kowalik, L. M. Tolbert, and J. Z. Zhang, J. Electroanal. Chem. **522**, 40 (2002).
[13] W. J. E. Beek, M. J. Wienk, and R. A. J. Janssen, Adv. Mater. (Weinheim, Ger.) **16**, 1009 (2004).
[14] K. M. Coakley, Y. Liu, M. D. McGehee, K. L. Frindell, and G. D. Stucky, Adv. Funct. Mater. **13**, 301 (2003).
[15] L. Kavan, J. Rathouský, M. Grätzel, V. Shklover, and A. Zukal, Microporous Mesoporous Mater. **44–45**, 653 (2001).
[16] P. D. Yang, D. Y. Zhao, D. I. Margolese, B. F. Chmelka, and G. D. Stucky, Nature (London) **396**, 152 (1998).
[17] G. J. de A. A. Soler-Illia, C. Sanchez, B. Lebeau, and J. Patarin, Chem. Rev. (Washington, D.C.) **102**, 4093 (2002).
[18] G. J. de A. A. Soler-Illia and C. Sanchez, New J. Chem. **24**, 493 (2000).
[19] E. L. Crepaldi, G. J. de A. A. Soler-Illia, D. Grosso, F. Cagnol, F. Ribot, and C. Sanchez, J. Am. Chem. Soc. **125**, 9770 (2003).
[20] L. Zhao, Y. Yu, L. Song, M. Ruan, X. Hu, and A. Larbot, Appl. Catal., A **263**, 171 (2004).
[21] A. Petrella, M. Tamborra, P. D. Cozzoli, M. L. Curri, M. Striccoli, P. Cosma, G. M. Farinola, F. Babudri, F. Naso, and A. Agostiano, Thin Solid Films **451–452**, 64 (2004).
[22] Z. Lin, D. H. Kim, X. Wu, L. Boosahda, L. LaRose, and T. P. Russell, Adv. Mater. (Weinheim, Ger.) **14**, 1373 (2002).
[23] F. S. Bates, Science **251**, 898 (1991).
[24] P. F. Green, T. M. Christensen, T. P. Russell, and R. Jerome, J. Chem. Phys. **92**, 1478 (1990).
[25] J. W. Kriesel, M. S. Sander, and T. D. Tilley, Chem. Mater. **13**, 3554 (2001).